

COMSOL Multiphysics: Application examples

Lecture 6

Special Topics:
Device Modeling

Outline

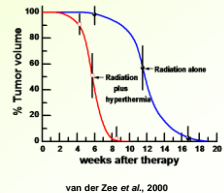
- Brief literature survey of problems/results
 - Biological systems and medical devices modeling
 - Food industry applications
 - PV applications
 - Plasmonic applications
- Hands on: running sample models

COMSOL Multiphysics capabilities

- Applicable to any problem that can be reduced to a system of PDE's
- Interface nodes guide through component and parameter input
- Different modules provide specialized interface and solvers; basic physics interfaces are available with the main program

Thermo-brachytherapy seed Med. Phys. project, G. Warrell et al.

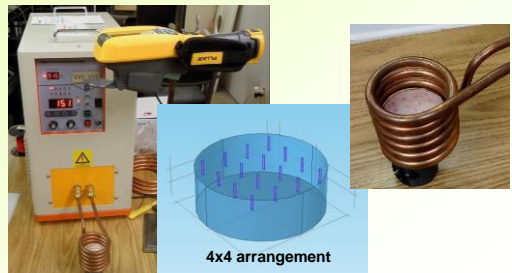
- Hyperthermia – defined as raising the temperature of tissue to 41 °C – 46 °C
- Use in combination with radiation enhances radiation effects on cancer cells and leads to large improvements in patient outcome
- Difficulties in attaining proper temperature range and uniformly heating deep-seated target volumes



Thermo-brachytherapy seed Med. Phys. project, G. Warrell et al.

- Proposed a combination implantable device (seed) serving as a source of radiation and heat when placed in oscillating magnetic field (induction heating)
- Generation and distribution of heat due to ferromagnetic cores is model with COMSOL
- For model verification conducted experiment with seed-sized pieces of ferromagnetic Ni-Cu alloy implanted into tissue-mimicking phantom (ham)
- Heated with 10 kW industrial induction heater; thermal data taken with fiber optic thermometer and infrared camera

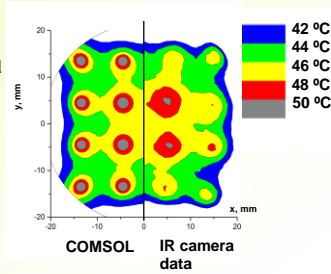
Thermo-brachytherapy seed Med. Phys. project, G. Warrell et al.



Thermo-brachytherapy seed

Med. Phys. project, G. Warrell et al.

- Modeled 2D temperature distribution compared with IR camera data
- Difference partially attributable to space-averaging in IR camera
- Blood perfusion rate BPR=0

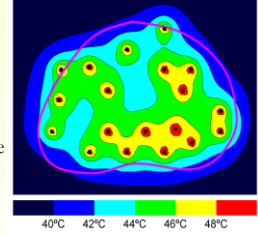


Thermo-brachytherapy seed

Med. Phys. project, G. Warrell et al.

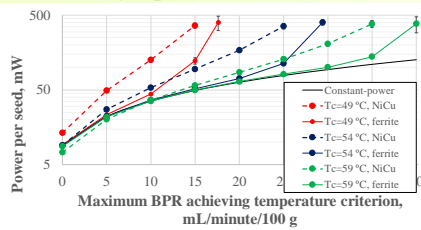
- Realistic distributions: 7 patients treated at UT
- Found the need for HT-only seeds to be placed in unused needle positions
- Included loss of heat in the target with uniform blood perfusion – full bioheat equation:

$$\rho_t C_t \frac{\partial T}{\partial t} - \vec{\nabla} \cdot (k \vec{\nabla} T) = Q_{ext} - \rho_b C_b \omega_b (T - T_b)$$



Thermo-brachytherapy seed

Med. Phys. project, G. Warrell et al.



- Model simplification: replace induction heating coupling with pure heat transfer model
- Calculated power production requirements vs. BPR

Towards understanding junction degradation in Cadmium Telluride solar cells,

Marco Nardone, J. Appl. Phys. 115, 234502 (2014)

- CdTe solar cell modeled with COMSOL for the first time
- Semiconductor module, introduced in ver. 4.4
- Employs an explicit time-dependent solver for this type of problem

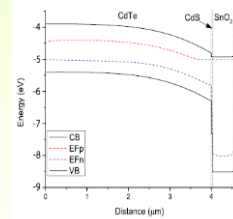


FIG. 1. Device structure and energy band diagram for the baseline cell under AM1.5G, 1 sun light at short circuit conditions. Energy is referenced to the vacuum level.

Towards understanding junction degradation in Cadmium Telluride solar cells,

Marco Nardone, J. Appl. Phys. 115, 234502 (2014)

- CdTe solar cell modeled with COMSOL for the first time
- Semiconductor module, introduced in ver. 4.4
- Employs an explicit time-dependent solver for this time-dependent degradation problem (not available with AMPS or SCAPS)
- Extensions to 2D and 3D are also possible

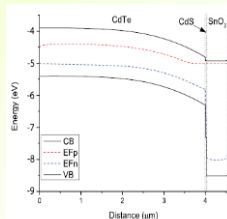


FIG. 1. Device structure and energy band diagram for the baseline cell under AM1.5G, 1 sun light at short circuit conditions. Energy is referenced to the vacuum level.

Towards understanding junction degradation in Cadmium Telluride solar cells,

Marco Nardone, J. Appl. Phys. 115, 234502 (2014)

- Defects are generated under light or bias in response to non-equilibrium charge carriers
- Defect generation rate $\frac{dN}{dt} = \alpha n - \beta n$
- N – defect concentration, n – charge carrier (e- or holes) concentration, α and β are material parameters

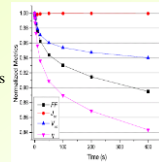


FIG. 7. Dependence of defect concentration on time for the model of Fig. (1) with generation and recombination rates of charge carriers by the illumination of the cell with 1 sun light. The generation conditions are as in Fig. (1) and the recombination rates are $\alpha = 10^{-10}$ s⁻¹ and $\beta = 10^{-10}$ s⁻¹.

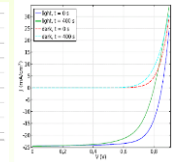


FIG. 8. Recombination and production (R) curves for the model of Fig. (1). Same conditions as for Fig. (7). The recombination conditions are as in Fig. (1) and the generation rates are $\alpha = 10^{-10}$ s⁻¹ and $\beta = 10^{-10}$ s⁻¹.

- Junction degradation consisting of self-compensatory defect evolution in response to the presence of excess charge carriers leads to commonly observed degradation modes

Shading-induced failure in thin-film photovoltaic modules: Electrothermal simulation with nonuniformities
 M. Nardone, S. Dahal, and J. Waddle, manuscript submitted

- Investigate shading-induced failure in thin-film modules using *electro-thermal* numerical simulation
- Non-uniformity modeling in PV modules approached before with SPICE
- The ability of FEM to easily include localized variations with increased mesh refinement is essential

Individual cells in a module are connected in parallel

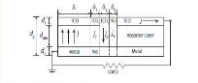


FIG. 1. Modifiable module schematic of one interconnect section. Dashed lines indicate current direction, not material breaks. INS is insulating material. Light is incident from the top. This schematic is a simplified representation of a typical substrate configuration device, such as commercial CIGS.

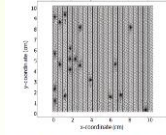


FIG. 4. Meshed details of a thin-film module with 20 non-uniformly placed points of nonuniformity.

Shading-induced failure in thin-film PV modules
 M. Nardone, et al.

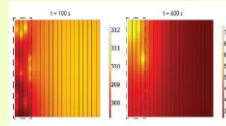


FIG. 6. Temperature distributions (in K) in a 20% shaded, unsegmented mini-module with 20 non-ohmic shunts ($\alpha = 6$ in Fig. 3) at 100 s and 600 s after turning on the light source of 1000 W/m^2 intensity. Dashed box delineates shaded region. Note the difference in scales.

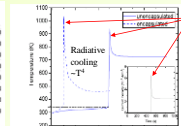


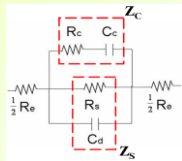
FIG. 7. Maximum module temperature as a function of time. Horizontal dashed line indicates temperature at each event. Inset: maximum current density in the PV cell as a function of time.

Runaway point due to joule heating; leads to material damage and ohmic shunt formation

- Simulations replicate most experimental observation for shaded modules, including predictions of explosive events
- The kinetic mechanism is based on weak spots with low reverse breakdown voltage; subsequent ohmic shunting results in significant performance loss under normal operating conditions

A systematic investigation into the electrical properties of single HeLa cells via impedance measurements and COMSOL simulations,
 M.-H. Wang, L.-S. Jang, Biosens. and Bioel. 24 (2009) 2830–2835

- The electrical properties of single cells provide fundamental insights into their pathological condition and enables the construction of functional cell models

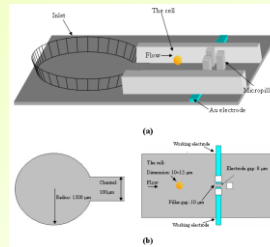


The circuit diagram of the impedance model

- Modeled with AC/DC module, utilizing equivalent circuit
- Based on the model empirical expressions to predict the conductivity and permittivity of single HeLa cells were found

HeLa is a cell line of immortal cancer cells harvested from Henrietta Lacks, a cervical cancer patient at Jones Hopkins clinic in 50's

A systematic investigation into the electrical properties of single HeLa cells



(a) 3D schematic of cell-trapping microstructure, (b) 2D schematic showing device dimensions.

- The impedance spectroscopy experiments were performed using HeLa cells suspended in a PBS buffer solution
- Cells were trapped in the microfluidic device and impedance properties were then measured at V from 0.1 to 1.0V and f in the range 1–100 kHz

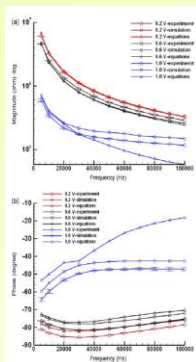


Fig. 3. Variation of (a) magnitude and (b) phase of HeLa impedance signals as obtained experimentally, numerically and analytically for operational voltages of 0.2, 0.4 and 1 V and operational frequencies in the range 1–100 kHz.

A systematic investigation into the electrical properties of single HeLa cells

- Close agreement between measured and simulated amplitude and phase values for the range of operating conditions were established
- Equations for conductivity and permittivity were found and successfully tested

Virtual Modeling of Thermo-Physiological Comfort in Clothing

P. Van Ransbeeck, R. Benoot, B. Van Der Smissen, COMSOL conference 2015

- The dynamic heat and moisture transmission characteristics of clothing
- The thermal functions of clothing are depending on the complex interactive physical behaviors involved in the clothing wearing system, which consists of (1) the human body, (2) the clothing and (3) the external environment
- Examined the flow and temperature distribution of clothed wearing systems including air gaps using Computational Fluid Dynamics (CFD) and Heat transfer modules

Virtual Modeling of Thermo-Physiological Comfort in Clothing

P. Van Ransbeeck, R. Benoot, B. Van Der Smissen, COMSOL conference 2015



Figure 1: Creation of virtual clothed manikin

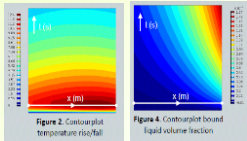


Figure 2: Contourplot temperature rise/fall

Figure 4: Contourplot bound liquid volume fraction

- Temperature raise/fall across a wool textile (porous medium) was modeled as coupled diffusion phenomena of heat and moisture
- Virtual 3D manikin will be developed next

Modeling and Simulation of Hydration Operation of Date Palm Fruits Using COMSOL Multiphysics

A. Lakoud, S. Curet, M. Hassouna, COMSOL conference 2015

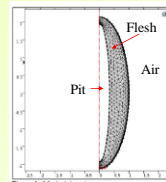


Figure 3: Meshed domain
2D-axial symmetry geometry

- Hydration is the key unit operation in the thermal process of dates
- Objective was the optimization of this operation in order to enhance the mass transfer at the surface and to reduce the energy consumption during hydration
- Use “Transport of diluted species” (under “Chemical Species Transport”)

Modeling and Simulation of Hydration Operation of Date Palm Fruits Using COMSOL

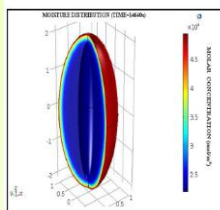


Figure 6: Moisture concentration distribution within date flesh after 4h

- The model allowed to estimate both moisture diffusivity and convective mass transfer coefficient; it was validated experimentally
- Results will be used for the hydration process optimization

Numerical Analysis on Plasmonic Nano-Cucumber Achieving Large EFs and Wide Tuneability of the Peak

A. Zare, E. Cutler, H. Cho, COMSOL conference 2015

- Surface plasmon resonance based on optical properties of metallic nanostructures can be used for detection of special biological targets, including individual molecules
- Gold nanostructures with different shapes and sizes have been designed to achieve high enhancement factor (EF), wide range of tuneability of the plasmonic peak

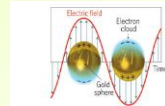


Figure 1: Collective oscillation of electrons with the incident electromagnetic field at a flat gold-air interface¹

- RF Module, Electromagnetic waves, Frequency Domain is chosen as the physics; Frequency Domain used as the study

Numerical Analysis on Plasmonic Nano-Cucumber Achieving Large EFs and Wide Tuneability of the Peak

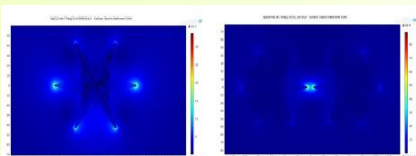


Figure 2: The cross section of single and coupled nanocucumbers. The main factors are introduced.

- The unique features of the nanocucumber makes it a strong candidate for the application of ultrasensitive detection of wide range of biological targets

Model for hands-on: Electrical Heating in a Busbar

- Extension of the electrical heating problem:
 - Add structural mechanics: solve for Joule heating and thermal expansion
 - Add cooling by airflow: solve for fluid flow and Joule heating
- Alternatively: start setting up your project

Summary

- COMSOL Multiphysics is a versatile commercial PDE solver
- Specific modules direct modeling process
- Well-developed run-time (through Excel, MatLab) and post-processing facilities

References

- Introduction to COMSOL Multiphysics, www.comsol.com
- W. B. J. Zimmerman, Multiphysics modelling with finite element methods, World Scientific, 2008
- Other references are provided within slides